Atom-Specific Probing of Electron Dynamics in an Atomic Adsorbate by Time-Resolved X-Ray Spectroscopy

Simon Schreck,[1] Elias Diesen,[2,*,†] Martina Dell'Angela,[3] Chang Liu,[1] Matthew Weston,[1] Flavio Capotondi,[4] Hirohito Ogasawara,[5] Jerry LaRue,[6] Roberto Costantini,[3,7] Martin Beye,[8] Piter S. Miedema,[8] Joakim Halldin Stenlid,[1,2] Jörgen Gladh,[1,5] Boyang Liu,[1] Hsin-Yi Wang,[1] Fivos Perakis,[1] Filippo Cavalca,[1] Sergey Koroidov,[1] Peter Amann,[1] Emanuele Pedersoli,[4] Denys Naumenko,[4] Ivaylo Nikolov,[4] Lorenzo Raimondi,[4] Frank Abild-Pedersen,[2] Tony F. Heinz,[5,9] Johannes Voss,[2] Alan C. Luntz,[2] and Anders Nilsson[1]

[1]*Department of Physics, AlbaNova University Center, Stockholm University, SE-10691 Stockholm, Sweden*
[2]*SUNCAT Center for Interface Science and Catalysis, SLAC National Accelerator Laboratory, 2575 Sand Hill Road, Menlo Park, California 94025, USA*
[3]*CNR-IOM, SS 14—km 163.5, 34149 Basovizza, Trieste, Italy*
[4]*FERMI, Elettra-Sincrotrone Trieste, SS 14—km 163.5, 34149 Basovizza, Trieste, Italy*
[5]*SLAC National Accelerator Laboratory, 2575 Sand Hill Road, Menlo Park, California 94025, USA*
[6]*Schmid College of Science and Technology, Chapman University, Orange, California 92866, USA*
[7]*Physics Department, University of Trieste, Via Valerio 2, 34127 Trieste, Italy*
[8]*Deutsches Elektronen-Synchrotron DESY, Notkestrasse 85, Hamburg 22607, Germany*
[9]*Department of Applied Physics, Stanford University, Stanford, California 94305, USA*

(Received 16 February 2022; revised 14 June 2022; accepted 18 November 2022; published 29 December 2022)

The electronic excitation occurring on adsorbates at ultrafast timescales from optical lasers that initiate surface chemical reactions is still an open question. Here, we report the ultrafast temporal evolution of x-ray absorption spectroscopy (XAS) and x-ray emission spectroscopy (XES) of a simple well-known adsorbate prototype system, namely carbon (C) atoms adsorbed on a nickel [Ni(100)] surface, following intense laser optical pumping at 400 nm. We observe ultrafast (∼100 fs) changes in both XAS and XES showing clear signatures of the formation of a hot electron-hole pair distribution on the adsorbate. This is followed by slower changes on a few picoseconds timescale, shown to be consistent with thermalization of the complete C/Ni system. Density functional theory spectrum simulations support this interpretation.

DOI: 10.1103/PhysRevLett.129.276001

Fundamental dynamical processes of adsorbates on surfaces, e.g., energy or charge transfer, desorption, etc., often define catalytic and especially photocatalytic activity and selectivity. These processes are typically in the femtosecond regime, where optical pump-probe experiments have been used to follow the adsorbate dynamics [1–3]. The optical pump excites high energy electron-hole (*e*-*h*) pairs in the metal which locally thermalize within ∼100 fs to create a quasiequilibrium, often described by a two temperature model (2*T*) with one high temperature for the *e*-*h* pairs and one for substrate phonons [4,5], with equilibration between the two systems occurring on a several picosecond timescale. Both modes can excite vibrations of adsorbates and therefore ultimately drive chemistry. The focus of laser-induced chemistry on metals has traditionally been on the relative role of substrate vibrations or electronic excitations in inducing chemical change [6]. Inferences regarding the electronic structure changes of adsorbates due to optical laser excitation of the supporting metal have only been *indirect*, based on what surface chemistry is induced [5]. However, *direct* experimental probing of the electronic structure changes due to the laser excitation on the adsorbate atoms themselves has been lacking.

Recently, with the emergence of x-ray free-electron lasers, optical pump–x-ray probe measurements of ultrafast surface chemistry have become possible. Since the x-ray spectroscopic probe can measure element-specific changes in the electron structure, much more detailed information about the chemistry occurring in the ultrafast time regime can be obtained than in pure optical pump-probe experiments. For example, it has been possible to detect a transient precursor state in CO desorption [7,8], a transient adsorbed CHO intermediate [9], the transition state region in CO oxidation [10], and ultrafast vibrational excitations in adsorbed CO on a Ru(0001) surface [11], as well as, e.g., elucidate photooxidation of CO on oxides [12]. However, in none of the previous work done at x-ray lasers has it been possible to detect electronic structure changes on the adsorbate prior to the nuclear dynamics. In contrast, for bulk metals direct x-ray probing of the excited electronic system has been achieved [13,14].

In this Letter, we aim to provide, in an atom-specific way, this missing information on direct changes of the

 © 2022 American Physical Society

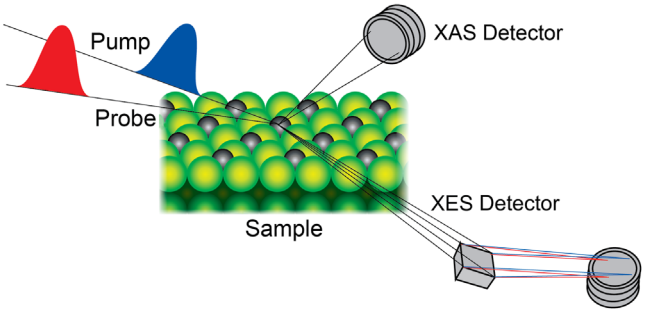

FIG. 1. A 400 nm pump laser and a soft x-ray probe laser beam are incident at grazing angle to the C/Ni(100) surface. The two beams arrive at different times allowing for pump-probe measurements. The XAS detector detects all emitted photons in a large solid angle whereas the XES detector contains an energy-dispersive soft x-ray spectrometer. In XAS the incoming photon energy is scanned whereas in XES it is fixed to allow for specific excitations.

adsorbate electronic structure caused by an optical pulse. We choose a most simple, strongly adsorbed atomic system where the electronic structure is well understood in terms of the d-band model, which describes the simple adatom $2p$ interaction with the metal states leading to bonding and antibonding adatom $2p$–metal d states [15]. With x-ray spectroscopy the projection on the adsorbate atom [16] of the bonding and antibonding states can be directly experimentally probed, providing an opportunity for a fundamental picture of optical laser induced changes. The carbon adsorbate is a prototypical strongly bonded atomic adsorbate that is well characterized with x-ray spectroscopy-based synchrotron radiation measurements because of its relatively narrow linewidths [17,18]. Here, we directly follow the changes in the occupied and unoccupied local states of a strongly adsorbed C atom, using x-ray absorption spectroscopy (XAS) and x-ray emission spectroscopy (XES) after intense laser excitation (at 400 nm) of a Ni(100) substrate. With the usage of externally seeded x-ray laser beams [19], it is possible to probe the adsorbate electronic structure dynamics with a time resolution of $\approx$100 fs. We observe both ultrafast ($\sim$100 fs) changes in the C x-ray spectra and slower changes occurring on a picosecond timescale. Both electronic and nuclear excitations of C thus affect the x-ray spectra, and these excitations are analyzed theoretically.

Figure 1 shows the principles of core-level excitation (XAS) and deexcitation (XES) allowing for element-specific probing of the electronic structure in both the occupied (XES) and unoccupied (XAS) states through the involvement of the strongly localized C $1s$ level [17]. The measured spectra reflect the projected density of states of C $2p$ character through the dipole selection rule for a $1s$-$2p$ transition. To obtain a temporally well-controlled probe of soft x-ray pulses relative to the optical pump, a seeded x-ray laser was used from the FERMI facility [20]. The sample is adsorbed C on Ni(100) (coverage 0.5 ML) that has been structurally characterized as a $p4g$ overlayer [21] with the C atoms fourfold coordinated by Ni atoms in a hollow site and with the C almost within the first Ni layer [22]. The 400 nm (3.1 eV photon energy) optical pump laser, with a focus of $\sim 150 \times 150$ μm^2 and a pulse energy of $\sim$152 μJ, arrives at the sample, followed by the soft x-ray probe at variable time delays. The C atom probing is performed with XAS using a fluorescence detector and with XES using a soft x-ray spectrometer. XAS and XES studies of C/Ni have shown relatively narrow spectral profiles allowing observation of detailed changes [23]. Details on the experimental method are found in Supplemental Material [24].

Figure 2(a) shows the C K-edge XAS at different delay times. The electric field (E) vector is parallel to the surface, meaning the XAS probes unoccupied orbitals of local C $2p$ character oriented parallel to the surface. The spectrum at -0.4 ps delay (i.e., before the pump pulse) can be directly compared to XAS of the same system measured with synchrotron radiation, where the photon energy has been calibrated on an absolute scale [18]. This gives the energy scale in Fig. 2(a). For adsorbates on metallic systems, the onset of the XAS corresponds to the Fermi level, so that the core-level binding energy can be used to reference the XAS onset [18,58,59]. The XPS-determined C $1s$ binding energy of C on Ni(100) is 283.0 eV and is indicated with an arrow in Fig. 2(a). The broad peak in the XAS spectrum that is above the XPS binding energy position can be related to the Ni $3d$–C $2p$ antibonding resonance [15–17]. The weak structure around 282 eV is due to imperfect background subtraction.

The XAS spectrum at 0.3 ps delay shows two significant changes: increased intensity below 283 eV [orange region in Fig. 2(a)], and reduced intensity above 283 eV (turquoise region). The use of the C K-edge XAS directly implies that the observed changes occur in the electronic structure on the adsorbed C atoms. These two changes are diminished in the spectrum at 1.2 ps delay and instead additional intensity is seen in the region 284–285 eV (gray region). At 4.0 ps delay the spectrum is nearly identical to that at 1.2 ps.

Figure 2(b) shows C K-edge XES spectra generated with an incoming photon energy of 284 eV with the E vector parallel to the surface and the emitted soft x rays detected at a grazing angle with respect to the surface. With grazing emission we probe the occupied C $2p$-derived orbitals both parallel and perpendicular to the surface [17]. The emission energy scale for the spectrum at negative delay is calibrated by comparison with XES from synchrotron radiation [17]. At -0.5 ps delay the spectrum consists of a broad main peak centered around 278.5 eV with a clear asymmetry to higher energies and a cutoff at 283 eV corresponding to the Fermi level. The main peak is associated with the Ni $3d$–C $2p$ bonding resonance. After laser excitation at 0.2 ps delay we observe three different changes in the XES spectrum,

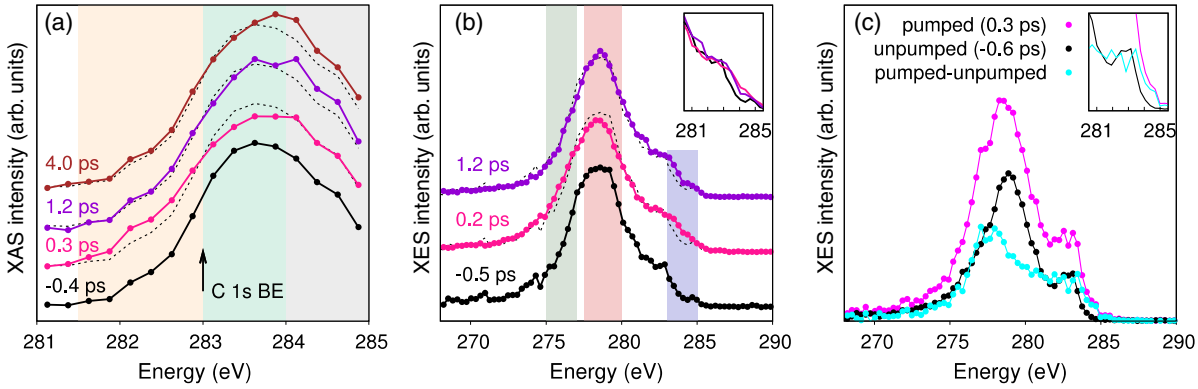

FIG. 2. Experimental XAS and XES spectroscopy of C/Ni(100). (a) XAS spectra measured with the E vector parallel to the surface at different delay times between the optical and soft x-ray laser beams. The arrow indicates the C 1s binding energy used for calibration. (b) XES spectra in grazing emission using an excitation energy of 284 eV. (c) Resonant excited XES spectra at a photon energy of 282.5 eV with negative delay and 0.3 ps delay, and the difference spectrum between the two. The insets in (b) and (c) show an enlarged region around the C 1s core-level binding energy corresponding to the Fermi level of the system. The color coding in (a) and (b) indicates regions where spectral intensity variations with delay time are shown in Fig. 3.

(i) the main peak at 278.5 eV loses some intensity (red region), (ii) there is small additional intensity appearing between 275–277 eV (green region), and (iii) additional intensity above the Fermi level at 283 eV (blue region). These changes vanish in the 1.2 ps delay spectrum, except for a small intensity increase still remaining above 283 eV. It is important to note that the changes around the main peak (i) and below (ii) correspond to electronic states that are too far below the Fermi level to be energetically accessible for a single-photon excitation from the 400 nm (3.1 eV) laser light.

Figure 2(c) shows XES spectra at 0.3 ps delay and for the unpumped case (−0.6 ps delay) after x-ray excitation to 282.5 eV, i.e., 0.5 eV below the Fermi edge. In the unpumped spectrum, the intensity in this (nominally Pauli blocked) region is due to phonon, core-hole lifetime, and instrumental broadening of the XAS spectrum, giving rise to a low-energy tail [18]. Both spectra are normalized by the incoming fluence; the total intensity therefore increases after pumping, corresponding to the increased XAS intensity at 282.5 eV at 0.3 ps delay. The difference spectrum between the pumped and unpumped corresponds to selective probing of atoms where holes have been generated below the Fermi level by the 400 nm laser excitation increasing the overall x-ray absorption cross section and thereby the total XES intensity. We observe in the difference XES spectrum that the main peak is shifted from 279 to 277.5 eV, and additional intensity appears above the Fermi level. This is consistent with the XES spectral changes due to the laser pump shown in Fig. 2(b), but more enhanced since the selective x-ray excitation leads to a decreased background signal from nonexcited species.

Figure 3 shows the time traces from the spectral changes in Figs. 2(a) and 2(b). Starting with the XAS time-dependent changes shown in Fig. 3(a), we observe changes for both the holes (orange) and electrons (turquoise) at 0.25 ps with an apparent Gaussian rise time of around 0.1 ps, and with a slower recovery of around 0.2 ps. There is a delayed onset of around 0.15 ps as determined by the Gaussian rise half maximum. The long-term spectral change (gray) is delayed until 0.5 ps with a rise time of 0.2 ps with no detectable recovery within the measured 4.0 ps. The XES spectral changes around the main peak (green and red) appear to be faster with the onset at almost 0 ps and with a slightly faster rise time; the recovery time of ∼0.25 ps appears somewhat slower than in the XAS. Both the XAS and XES rapid changes have decayed within 0.5 ps. The changes above the Fermi level (blue) in the XES

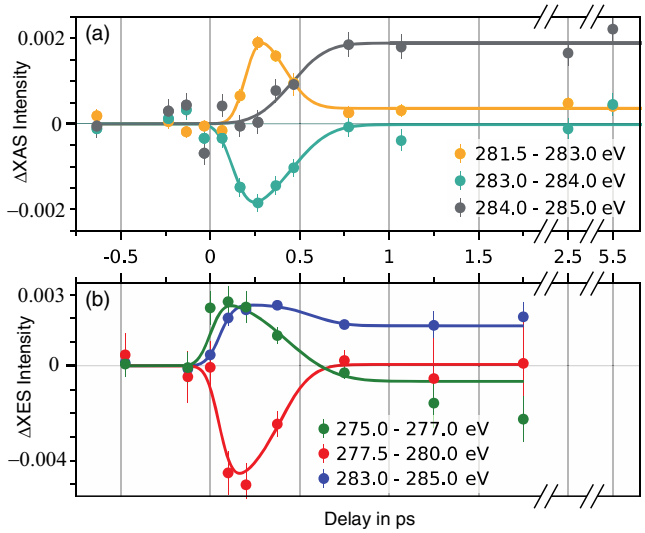

FIG. 3. XAS and XES spectral regional integrated difference intensity of different delay times. (a) XAS time traces and (b) XES time traces (excitation at 284 eV). The color of each time trace represents different spectral regions indicated in Fig. 2. Note that these regions are not the same for XAS and XES.

spectra have an onset of 0.1 ps and then remain, similar to the long-term time component in the XAS. We note that the XAS and XES data were not measured simultaneously and it is not possible to exclude timing drift defining the temporal overlap of the optical and x-ray beam (t_0) over 24 h, so that uncertainties in defining $t_0 \sim \pm 0.1$ ps are realistic.

In order to assist in the interpretation of the experimental data we have computed x-ray spectra with both electronic and nuclear excitations. This was done by density functional theory calculations at the generalized-gradient approximation (GGA) level using the QUANTUM ESPRESSO [60,61] code, with spectra calculated using the XSPECTRA [62–64] code. Details on the method are found in Supplemental Material [24]. Calculation of the frequency-dependent dielectric constant for the C/Ni system relative to the pure Ni metal indicate minimal optical absorption in the C relative to that in the Ni metal (see Supplemental Material [24]) so that all electronic structure changes of the C is a result of excitations in the Ni substrate. For the optical fluence used, the $2T$ model gives a peak electronic temperature of $T_e \approx 5000$ K within ~100 fs of the optical laser excitation, followed by a surface equilibration to $T \approx 1000$ K after ~2 ps via electron-phonon coupling (for details see Supplemental Material [24]). By comparing with measurements on other transition metals [65,66], we assume that thermalization of the hot electrons and holes occurs on a timescale of ~100 fs.

Figure 4(a) shows the calculated XAS from the ground state and excited systems corresponding to a high electronic temperature $T_e = 5000$ K and a fully thermalized system at $T = 800$ K. The effect of high T_e on the calculated XAS is twofold. The absorption onset, which at 0 K can be identified with E_F, is shifted (see Supplemental Material, Fig. S3 [24]). In addition, the broad Fermi-Dirac distribution at high T_e means that states well above E_F are populated, thus lowering the XAS intensity which probes unoccupied states. Since we have populated electronic states above the Fermi level, as indicated by the XAS, we should also observe these in the occupied states as probed by XES. Indeed the 5000 K electron distribution of the XES spectra shown in Fig. 4(b) shows intensity appearing above the Fermi level.

The appearance of intensity below E_F and a decreased intensity above E_F is consistent with the experimental XAS at early time as shown in Fig. 2(a). We therefore find that the features of the experimental XAS at $t = 0.2$ ps are all qualitatively reproduced in the theoretical spectra by simply considering the hot e-h pair distribution on the C. While the observation (and thermalization) of a hot e-h pair distribution in bulk metals has been extensively studied via two-photon photoemission studies [65,66] and time-resolved XAS [14,67], here we show the direct observation of this in an adsorbate.

The increase at the high-energy side of the main XAS peak at 4 ps delay is qualitatively reproduced in the

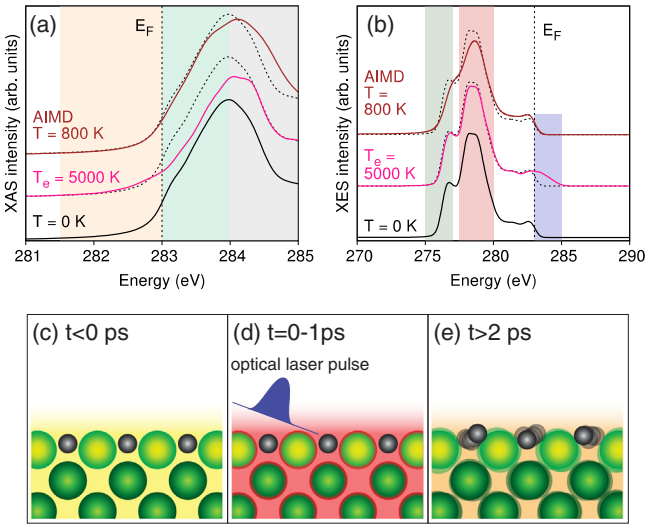

FIG. 4. Computed XAS (a) and XES (b) spectra. The black lines show the vibrational ground state spectra; the brown line shows the result from an *ab initio* molecular dynamics (AIMD) simulation at 800 K; and the pink line shows the result of a high electronic temperature. (c)–(e) Schematic summary of the findings. (c) At $t < 0$, before the optical laser excitation, carbon atoms (black spheres) are adsorbed in hollow sites on the nickel (100) substrate, in which a lattice of positively charged nickel ions (green spheres) share free electrons (shaded yellow region). (d) At $t = 0$, the optical laser pulse excites electrons in the metal to produce hot electrons (shaded red region). (e) The hot electrons lose their energy to substrate phonons and raise the temperature of the adsorbate-substrate system.

simulation of the spectrum from a fully thermalized system at 800 K, as shown by the curve labeled AIMD in Fig. 4(a). The increasing intensity in this region is consistent with thermal motion of C atoms towards lower coordinated bonding geometries than the fourfold hollow sites they occupy initially (Supplemental Material, Fig. S4 [24]). We observe that the excited e-h population seen in the experimental XAS decays on a timescale of ~300 fs, simultaneous with an increase in the intensity ~1 eV above E_F. Thus, these spectral changes are consistent with a decreasing electronic temperature via electron-phonon coupling and corresponding heating of the phonon modes, and is in good agreement with the timescales of the $2T$ model for Ni (Supplemental Material, Fig. S2 [24]). In the XES we also observed a similar decay of the intensity around E_F but it does not return to the intensity prior to the pump. This is most likely related to the broadening and shift of the Fermi level at the equilibrated 800 K temperature.

In addition to these effects, the experimental XES spectrum shows some redistribution of intensities in the main peak [Figs. 2(b) and 2(c)] at 0.3 ps delay, that cannot be explained by simply a high T_e since these changes occur far below E_F. They decay on similar timescales as the holes and electrons in the XAS, indicating that these XES

changes are also related to the high electronic temperature. One possibility is that extremely strong nonadiabatic coupling occurs to the parallel vibration of C on the Ni lattice (see Supplemental Material [24]). Ultrafast vibrational excitation (~0.1 ps) has been observed previously [11,68,69], although this is not well explained through conventional coupling via electronic frictions which predicts slower vibrational excitations. Another possibility is that many-body or demagnetization effects [70–72] in this highly excited electronic system could affect the width and position of the resonance, and ultimately cause the main XES line shape changes far from E_F in the short time regime. The XES depends sensitively on the two-dimensional band structure [73], where intensity of C character could be redistributed between different critical points in the Brillouin zone to cause the XES spectral change, and as the simulations indicate parallel C excitation does induce such a redistribution.

In conclusion, we have obtained XAS and XES of an atomic surface adsorbate with a well understood ground state electronic structure using a pump-probe scheme with an intense femtosecond 400 nm laser pulse as pump and a femtosecond x-ray pulse as probe. The simultaneous measurement of x-ray absorption and emission spectra reveals details of the dynamics on distinct timescales, as summarized in Figs. 4(c)–4(e). We see a direct effect on both XAS and XES of the initially high electronic temperature, which manifests itself as clearly identifiable changes in the line shape close to the Fermi level and only persists during the first picosecond. We can identify this as the timescale of thermal electronic excitation. Our observation constitutes direct experimental evidence that ultrafast laser excitation immediately leads to a highly excited *e-h* pair distribution not just in the substrate, but also in the adsorbate. The XAS high-energy shoulder at longer delays is a clear signature of a high overall temperature, and its gradual buildup indicates equilibration of the system, which takes place over several picoseconds. We identify this timescale as that of phonon excitation and the response of all substrate degrees of freedom to the excitation pulse. We also observe an immediate short time redshift of the main XES peak where the mechanism is more elusive. It could be due to ultrafast excitation of in-plane adsorbate vibrations but also many-body effects in the electronic system itself. This would give a third timescale associated with nonthermal electron-hole pairs and highly selective adsorbate excitation far from equilibrium conditions. Our results underscore the importance of taking high electronic temperature into account when studying, e.g., adsorbate dynamics or excitation spectra within a few picoseconds after intense optical pumping. Furthermore, the impact of how the adsorbate electron systems respond to optical stimuli could bring insights into photothermal catalysis, as recently observed for Ni nanoparticles on SiO_2 for sustainable fuel production [74].

This research was supported by the U.S. Department of Energy, Office of Science, Office of Basic Energy Sciences, Chemical Sciences, Geosciences, and Biosciences Division, Catalysis Science Program to the Ultrafast Catalysis FWP 100435 at SLAC National Accelerator Laboratory under Contract No. DE-AC02-76SF00515, Knut and Alice Wallenberg Foundation under Grant No. 2016.0042, the Swedish Research Council under Grant No. 2013-8823, U.S. This research used resources of the National Energy Research Scientific Computing Center, a DOE Office of Science User Facility supported by the Office of Science of the U.S. Department of Energy under Contract No. DE-AC02-05CH11231. The authors acknowledge the continuous support of the FERMI team during the setting up and operation of the FEL source for the experiment. M. B. and P. S. M. acknowledge funding from the Helmholtz association (VH-NG-1005). M. D. A. and R. C. acknowledge support from the SIR Grant No. SUNDYN [Nr RBSI14G7TL, CUP B82I15000910001] of the Italian MIUR. Part of the calculations were performed using resources provided by the Swedish National Infrastructure for Computing (SNIC) at the HPC2N and NSC centers. We acknowledge valuable discussions with Lars G. M. Pettersson.

S. S. and E. D. contributed equally to this work.

*Present address: Fritz-Haber-Institut der Max-Planck-Gesellschaft, Faradayweg 4-6, D-14195 Berlin, Germany.
†diesen@fhi.mpg.de

[1] F. Budde, T. F. Heinz, M. M. T. Loy, J. A. Misewich, F. De Rougemont, and H. Zacharias, Phys. Rev. Lett. **66**, 3024 (1991).
[2] H. Petek, H. Nagano, M. J. Weida, and S. Ogawa, J. Phys. Chem. B **105**, 6767 (2001).
[3] M. Bonn, C. Hess, S. Funk, J. H. Miners, B. N. J. Persson, M. Wolf, and G. Ertl, Phys. Rev. Lett. **84**, 4653 (2000).
[4] S. I. Anisimov, B. L. Kapeliovich, and T. L. Perel'man, Zh. Eksp. Teor. Fiz. **66**, 776 (1974) [Sov. Phys.-JETP **39**, 375 (1974)].
[5] C. Frischkorn and M. Wolf, Chem. Rev. **106**, 4207 (2006).
[6] M. Bonn, S. Funk, C. Hess, D. N. Denzler, C. Stampfl, M. Scheffler, M. Wolf, and G. Ertl, Science **285**, 1042 (1999).
[7] M. Dell'Angela *et al.*, Science **339**, 1302 (2013).
[8] H.-Y. Wang *et al.*, Phys. Chem. Chem. Phys. **22**, 2677 (2020).
[9] J. Larue *et al.*, J. Phys. Chem. Lett. **8**, 3820 (2017).
[10] H. Öström *et al.*, Science **347**, 978 (2015).
[11] E. Diesen *et al.*, Phys. Rev. Lett. **127**, 016802 (2021).
[12] M. Wagstaffe *et al.*, ACS Catal. **10**, 13650 (2020).
[13] C. Stamm *et al.*, Nat. Mater. **6**, 740 (2007).
[14] D. J. Higley *et al.*, Nat. Commun. **10**, 5289 (2019).
[15] B. Hammer and J. K. Nørskov, Nature (London) **376**, 238 (1995).
[16] A. Nilsson, L. G. M. Pettersson, B. Hammer, T. Bligaard, C. H. Christensen, and J. K. Nørskov, Catal. Lett. **100**, 111 (2005).

[17] A. Nilsson and L. G. M. Pettersson, Surf. Sci. Rep. **55**, 49 (2004).
[18] E. O. F. Zdansky, A. Nilsson, H. Tillborg, O. Björneholm, N. Mårtensson, J. N. Andersen, and R. Nyholm, Phys. Rev. B **48**, 2632 (1993).
[19] P. Finetti *et al.*, Phys. Rev. X **7**, 021043 (2017).
[20] E. Allaria *et al.*, Nat. Photonics **6**, 699 (2012).
[21] J. H. Onuferko, D. P. Woodruff, and B. W. Holland, Surf. Sci. **87**, 357 (1979).
[22] M. Bader, C. Ocal, B. Hillert, J. Haase, and A. M. Bradshaw, Phys. Rev. B **35**, 5900 (1987).
[23] A. Nilsson and N. Mårtensson, Phys. Rev. Lett. **63**, 1483 (1989).
[24] See Supplemental Material at http://link.aps.org/supplemental/10.1103/PhysRevLett.129.276001 for details on optical absorption in C/Ni; the two-temperature model; experimental methods; computational methods; XAS from different adsorbate geometries; and discussion of selective vibrational excitation, which includes Refs. [25–57].
[25] M. Gajdoš, K. Hummer, G. Kresse, J. Furthmüller, and F. Bechstedt, Phys. Rev. B **73**, 045112 (2006).
[26] G. K. White, Int. J. Thermophys. **9**, 839 (1988).
[27] Z. Lin, L. V. Zhigilei, and V. Celli, Phys. Rev. B **77**, 075133 (2008).
[28] D. Novko, J. C. Tremblay, M. Alducin, and J. I. Juaristi, Phys. Rev. Lett. **122**, 016806 (2019).
[29] A. P. Caffrey, P. E. Hopkins, J. M. Klopf, and P. M. Norris, Microscale Thermophys. Eng. **9**, 365 (2005).
[30] S.-S. Wellershoff, J. Güdde, J. Hohlfeld, J. G. Müller, and E. Matthias, Proc. SPIE Int. Soc. Opt. Eng. **3343**, 378 (1998).
[31] I. A. Abrikosov, A. V. Ponomareva, P. Steneteg, S. A. Barannikova, and B. Alling, Curr. Opin. Solid State Mater. Sci. **20**, 85 (2016).
[32] W. You *et al.*, Phys. Rev. Lett. **121**, 077204 (2018).
[33] P. Scheid, G. Malinowski, S. Mangin, and S. Lebègue, Phys. Rev. B **99**, 174415 (2019).
[34] T. Katayama *et al.*, J. Electron Spectrosc. Relat. Phenom. **187**, 9 (2013).
[35] L. Triguero, L. G. M. Pettersson, and H. Ågren, Phys. Rev. B **58**, 8097 (1998).
[36] E. Diesen, G. L. S. Rodrigues, A. C. Luntz, F. Abild-Pedersen, L. G. M. Pettersson, and J. Voss, AIP Adv. **10**, 115014 (2020).
[37] A. Nilsson *et al.*, Chem. Phys. Lett. **675**, 145 (2017).
[38] H. Öberg *et al.*, Surf. Sci. **640**, 80 (2015).
[39] B. Hammer, L. B. Hansen, and J. K. Nørskov, Phys. Rev. B **59**, 7413 (1999).
[40] S. Mallikarjun Sharada, R. K. B. Karlsson, Y. Maimaiti, J. Voss, and T. Bligaard, Phys. Rev. B **100**, 035439 (2019).
[41] D. Vanderbilt, Phys. Rev. B **41**, 7892 (1990).
[42] M. Leetmaa, M. P. Ljungberg, A. Lyubartsev, A. Nilsson, and L. G. M. Pettersson, J. Electron Spectrosc. Relat. Phenom. **177**, 135 (2010).
[43] A. Föhlisch, J. Hasselström, P. Bennich, N. Wassdahl, O. Karis, A. Nilsson, L. Triguero, M. Nyberg, and L. Pettersson, Phys. Rev. B **61**, 16229 (2000).
[44] G. Kresse and J. Furthmüller, Phys. Rev. B **54**, 11169 (1996).
[45] G. Kresse and J. Furthmüller, Comput. Mater. Sci. **6**, 15 (1996).
[46] G. Kresse and D. Joubert, Phys. Rev. B **59**, 1758 (1999).
[47] P. E. Blöchl, O. Jepsen, and O. K. Andersen, Phys. Rev. B **49**, 16223 (1994).
[48] J. J. Mortensen, L. B. Hansen, and K. W. Jacobsen, Phys. Rev. B **71**, 035109 (2005).
[49] J. Enkovaara *et al.*, J. Phys. Condens. Matter **22**, 253202 (2010).
[50] S. Flügge, *Practical Quantum Mechanics* (Springer-Verlag Berlin Heidelberg, 1971).
[51] S. Baroni, S. de Gironcoli, A. Dal Corso, and P. Giannozzi, Rev. Mod. Phys. **73**, 515 (2001).
[52] M. Calandra and F. Mauri, Phys. Rev. B **71**, 064501 (2005).
[53] M. Wierzbowska, S. de Gironcoli, and P. Giannozzi, arXiv:cond-mat/0504077.
[54] D. Menzel and R. Gomer, J. Chem. Phys. **41**, 3311 (1964).
[55] P. A. Redhead, Can. J. Phys. **42**, 886 (1964).
[56] J. A. Misewich, T. F. Heinz, and D. M. Newns, Phys. Rev. Lett. **68**, 3737 (1992).
[57] J. Gavnholt, T. Olsen, M. Engelund, and J. Schiøtz, Phys. Rev. B **78**, 075441 (2008).
[58] A. Nilsson, J. Electron Spectrosc. Relat. Phenom. **126**, 3 (2002).
[59] A. Nilsson, O. Björneholm, E. O. F. Zdansky, H. Tillborg, N. Mårtensson, J. N. Andersen, and R. Nyholm, Chem. Phys. Lett. **197**, 12 (1992).
[60] P. Giannozzi *et al.*, J. Phys. Condens. Matter **21**, 395502 (2009).
[61] P. Giannozzi *et al.*, J. Phys. Condens. Matter **29**, 465901 (2017).
[62] M. Taillefumier, D. Cabaret, A.-M. Flank, and F. Mauri, Phys. Rev. B **66**, 195107 (2002).
[63] C. Gougoussis, M. Calandra, A. P. Seitsonen, and F. Mauri, Phys. Rev. B **80**, 075102 (2009).
[64] O. Buñau and M. Calandra, Phys. Rev. B **87**, 205105 (2013).
[65] E. Knoesel, A. Hotzel, and M. Wolf, Phys. Rev. B **57**, 12812 (1998).
[66] M. Lisowski, P. A. Loukakos, U. Bovensiepen, J. Stähler, C. Gahl, and M. Wolf, Appl. Phys. A **78**, 165 (2004).
[67] E. Principi *et al.*, Struct. Dyn. **3**, 023604 (2016).
[68] K.-i. Inoue, K. Watanabe, and Y. Matsumoto, J. Chem. Phys. **137**, 024704 (2012).
[69] K.-i. Inoue, K. Watanabe, T. Sugimoto, Y. Matsumoto, and T. Yasuike, Phys. Rev. Lett. **117**, 186101 (2016).
[70] E. Beaurepaire, J.-C. Merle, A. Daunois, and J.-Y. Bigot, Phys. Rev. Lett. **76**, 4250 (1996).
[71] B. Koopmans, G. Malinowski, F. Dalla Longa, D. Steiauf, M. Fähnle, T. Roth, M. Cinchetti, and M. Aeschlimann, Nat. Mater. **9**, 259 (2010).
[72] B. Y. Mueller, T. Roth, M. Cinchetti, M. Aeschlimann, and B. Rethfeld, New J. Phys. **13**, 123010 (2011).
[73] T. Wiell, J. Klepeis, P. Bennich, O. Björneholm, N. Wassdahl, and A. Nilsson, Phys. Rev. B **58**, 1655 (1998).
[74] M. Cai *et al.*, Nat. Energy **6**, 807 (2021).